SEMARAK ILMU PUBLISHING

Journal of Advanced Research in Fluid Mechanics and Thermal Sciences

Journal homepage:
https://semarakilmu.com.my/journals/index.php/fluid_mechanics_thermal_sciences/index
ISSN: 2289-7879

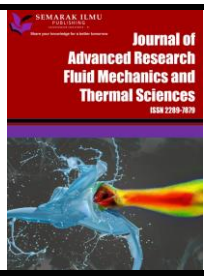

Experimental and CFD Resistance Validation of Naval Combatant DTMB 5415-51 Model

Alaaeldeen Mohamed Elhadad Ahmed[1,*], Ahmed Mokhtar Abo El-Ela[1]

[1] Shipbuilding Engineering Department, Military Technical College, Cairo, Egypt

ARTICLE INFO

Article history:
Received 30 March 2023
Received in revised form 13 June 2023
Accepted 20 June 2023
Available online 6 July 2023

Keywords:
DTMB; towing tank; resistance; CFD

ABSTRACT

The hull model of the surface combatant DTMB 5415 has been selected as a recommended benchmark naval ship for computational fluid dynamics (CFD) validation for resistance analysis. CFD is used to present a method for predicting surface combatant ship resistance. The resistance calculations of a 3 m DTMB 5415 hull model was compared using experimental and CFD techniques. The bare hull shape experiments were set up and carried out at the towing tank facilities at the Military Technical College's Hydrodynamic Laboratory in Egypt. A benchmark test will ensure that the equipment, procedures, and estimates of uncertainty are adequate. For the purpose of model validation, CFD calculations for a DTMB 5415-51 model are performed using three different mesh sizes for Froude numbers ranging from 0.10 to 0.40. For the same Froude numbers and free model conditions, results from towing tank experiments on the model's resistance, sinkage, and trim are presented. The numerical simulations are quantitatively consistent. The numerical results are compared in terms of wave field and resistance coefficients to determine the accuracy of the solution parameters. As evidenced by the resistance curves, the experimental investigation appears to provide very good agreement, indicating that the CFD model is capable of simulating the steady flow around a ship hull with acceptable accuracy and can thus be used as a supplement to laboratory model tests for ship design and ship hydrodynamic research.

1. Introduction

A newly constructed ship's resistance characteristics are often calculated numerically using various methods or tested via model testing in a towing tank. For the CFD validation of resistance and propulsion, a large benchmark database is available. The 22nd International Towing Tank Conference's Resistance Committee released a report on the thorough tests that went into building this database [1]. About 1980, the US Navy came up with the DTMB 5415 hull form at the David Taylor Model Basin (DTMB) as a concept for a surface combatant ship with a sonar dome bow and a transom stem [2].

* *Corresponding author.*
E-mail address: dr.aladdinahmed@gmail.com

https://doi.org/10.37934/arfmts.107.2.84102

For the verification, validation/calibration, and accreditation of computational fluid dynamics (CFD) codes in order to realize simulation-based design, particularly for contemporary hull forms, there is an ongoing demand for more model-scale data. When complicated fluid flow is present, CFD techniques are very helpful for studying flow issues in resistance prediction. While towing tank tests provide better absolute accuracy. Also, they have the benefit of enabling hull shape alterations, which provides a comparative examination of findings to be conducted in a reasonably short amount of time and at a quite low cost [3].

All the benchmark experimental data used to validate the CFD results were also gathered using the same hull model. It is clear that different choices of the parameters produce different flow prediction. Due to these factors, not only for the global values but also for the local features of the flow, an experimental validation of the computed results is required [4].

The present study provides the test results for the resistance, sinkage and trim for combatant surface ship model DTMB 5415-51 to a scale of λ = 51.2 in at the Military Technical College towing tank (MTC-TT). The resistance, sinkage and trim data has been performed following the ITTC standards for model speed (V_m) from 0.01 - 2.0 m/s equivalent to Froude numbers (Fr) 0.05-0.40. The results are repeated ten times for V_m = 0.5, 1.0, 1.5 and 2.00 m/s for checking accuracy. The results are discussed with regard to the data trends and compared to the CFD results.

This paper's requirement is to determine an accurate numerical prediction of hull model resistance, sinkage, and trim, as well as the flow field surrounding the hull model on various Froude number scenarios [5]. CFD results are as a primary step for production of a validated ship model then compared with experimental investigation in towing tank for model verification. The paper aim to compare the experimental results in MTC-TT with already documented results on DTMB 5415 3m Bench mark to ensure adequacy of laboratory setup ad procedures [6]. Results of the extensive experimental campaign are presented forming a benchmark for numerical methods validation.

2. Numerical Modelling

2.1 Hull Geometry

Many experimental and CFD test results for the surface combatant DTMB model 5415 are public and have been addressed at numerous workshops and conferences, including the Gothenburg, Tokyo, and SIMMAN workshops. Figure 1 and Table 1 provide a 3-D representation of the hull and the key details, which, when compared to the model tests from the David Taylor Model Basin in Washington, D.C., are accurate. The bare hull condition is used for computations and experimentation [7].

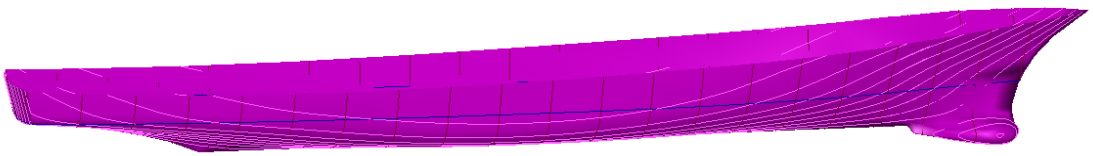

Fig. 1. DTMB #5415 Model geometry

Table 1
Main particulars of DTMB #5415 (ITTC, 2005)

L_{pp} (m)	2.78	Δ (kg)	63.5
B (m)	0.403	LCG (m)	1.375
D (m)	0.244	Wetted Surface Area (S) (m^2)	1.313
T (m)	0.120	Block Coefficient (C_B)	0.506

Figure 2(a) shows the body plan of DTMB model which is believed to be one of the best choices to simulate turbulence flow around ship hull. It is usually regarded as a preferred test sample to validate a new numerical method on this combatant hull [8] [9]. The grid structure and the profile of the combatant ship model corresponding to a scale of 51.10 used for CFD calculations are illustrated in Figure 2(b).

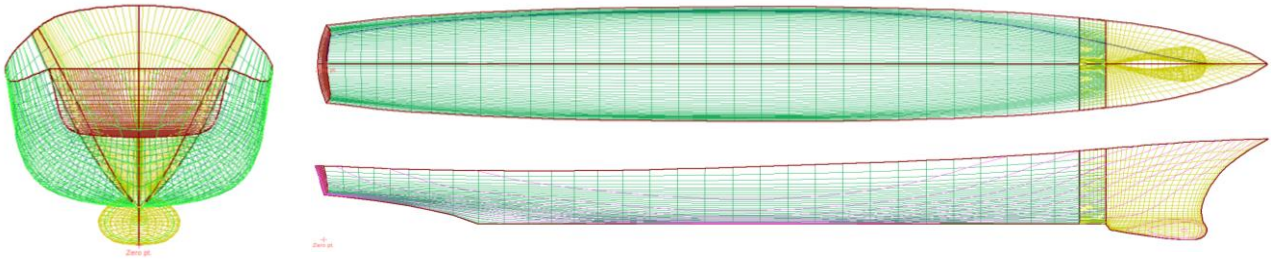

Fig. 2. (a) Body plan (b) Numerical grid of DTMB 5415 hull surface

2.2 Mathematical Model and Governing Equations

The continuity equation, in conjunction with the Reynolds-averaged Navier-Stokes (RANS) equations, can be used to represent the governing equations of an incompressible, two-phase (air and water), and viscous turbulent flow field. The SST k-ω Model was used to calculate the turbulent viscosity; further information on the model formulation and turbulence model equations is provided by Menter [10]. The VOF method is utilised to simulate multiphase free-surface flow.

The fluid domain is partitioned into a finite number of cells, and a discretionary process into algebraic form to be solved then converts the governing equations for fluid flow. A simple algorithm was used to achieve the coupling of the pressure and velocity fields The computation is carried out in Fluent, a multipurpose CFD software that was recently used to simulate ship flow [11]. In this study, we demonstrate that the calculation for ship resistance with varying Froude number can be undertaken in the Fluent as well.

2.3 Computational Domain, Boundaries and Mesh Configuration

The rectangular hull-meshed domain is separated into the water zone and the air zone. All analytical and numerical solutions must be applicable to the given boundary and initial conditions. These requirements need to be specified in accordance with the flow characteristics. The resistance behavior of the DTMB 5415 hull in deep water was predicted computationally in the current work. To reduce computational time, only half of the model conforming to the hull symmetry was modelled. Figure 3 displays the main hull's boundary conditions. While the flow velocity is taken to be equal to the experimental velocity of the model, the inlet and outlet boundary conditions upstream and downstream are taken as velocity inlet and pressure-outlet with an open channel, respectively. No-slip walls with zero normal and tangential velocities were used. As a result, both kinematic boundary condition and no-slip condition were satisfied on the hull surfaces [12]. Symmetry condition is invoked on the symmetric plane.

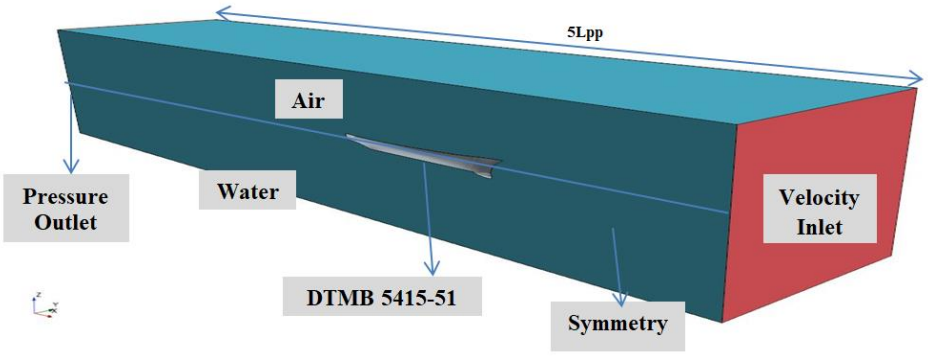

Fig. 3. Computational Domain and boundary conditions of the DTMB 5415-51

It should be observed that the main hull and the corresponding hulls with other scales are geometrically identical. The x, y, and z-axes are oriented with x-axis pointing towards the bow, y-axis to portside and positive z upwards and negative z downwards directions. Table 2 also provides the computational domain's dimensions.

Table 2
Computational domain Dimensions

Upstream	1.0 L_{OA}	front of the bow
Down stream	3.0 L_{OA}	from the stern
Top	0.5 L_{OA}	depth of air zone
Bottom	1.0 L_{OA}	depth of water zone
Transverse	1.0 L_{OA}	width of both zones

To create a structured multi-block grid, the domain volume is divided into several sub-volumes [13]. In order to acquire greater resolution of the free-surface elevation in the important area and improve the boundary layer approximation, the grids at the free surface and close to the model are refined. According to Figure 4, the minimum grid spacing away from the hull wall is 1×10^{-3} L_{PP}.

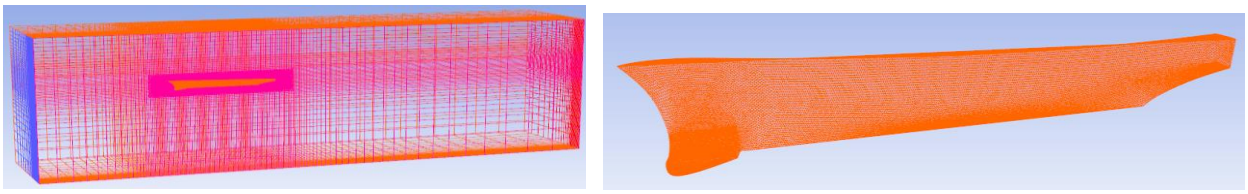

(a) (b)

Fig. 4. (a) Hull domain volume in gambit; (b) DTMB #5415 Model cells

Three main processes are necessary for a CFD solution: processing, problem analysis, and post-processing of the outcomes [14]. In our work, the suitable mesh production in the Gambit programme is combined with the development of the hull geometry as the solution. Figure 5 depicts the locations of the ship model relative to the various solution domain boundaries as well as a general perspective of the mesh surrounding the ship model. Over the entire solution domain, a hybrid structured/unstructured mesh with around 1.15 million cells was produced [15]. The computational domain was discretized using hexahedral components. Local grid refinements were used close to the free surface and around the hull. In this investigation, three different mesh sizes were examined with a total element count of 0.99 M, 1.45 M and 2.1 M for coarse, medium and fine grid respectively.

The calculations for this work were performed using the Fluent programme, which employs a hybrid-structured grid to solve the RANS equations using a finite-volume method [16] [17]. Gravity

effects must be included in boundary conditions because gravitational and inertial forces control the motion of the free surface. The calculations make use of the SST k-ω turbulence models with standard coefficients. Monitoring the residuals of continuity, velocity, turbulence, volume fraction, and drag force allows for the assessment of the solution's convergence. The assumed value for the residual convergence criterion is 1E-07 [18]. Froude numbers ranging from 0.1 to 0.45 were separately computed for various scenarios. The time step is Δt = 0.0001s.

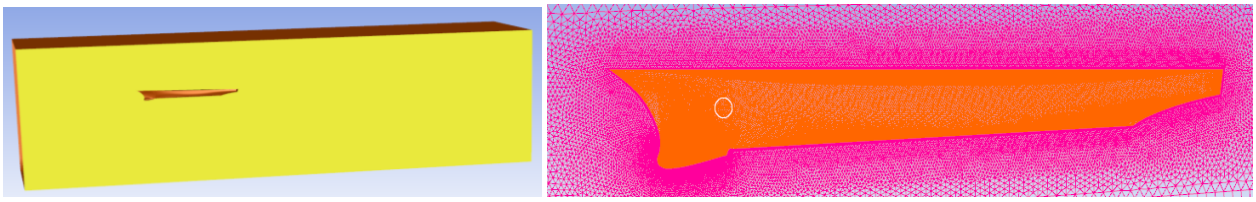

(a) (b)

Fig. 5. (a) Solution domain (b) Overall view of the mesh around the model ship

3. Experimental Setup

3.1 Description of the Facility and Equipment

The experiments have been carried out in the Hydrodynamic Laboratory at the Military Technical College, Cairo. The towing tank (MTC-TT) has the geometrical specifications; 45 m long, 5 m wide and has a water depth 3.8 m and technical specifications, which include a J-frame carriage with speed to 2 m/sec and carriage max payload of 50 kg. It is equipped with a complete wave maker system that includes eight multi-flap paddles designed and built by Edinburgh Designs Ltd. as seen in Figure 6. To stabilise operation and achieve the appropriate transfer function, the wavemaker uses force feedback mode in the electronic control system. Moreover, the wave maker incorporates absorption facilities to eliminate the impacts of reflected waves [19].

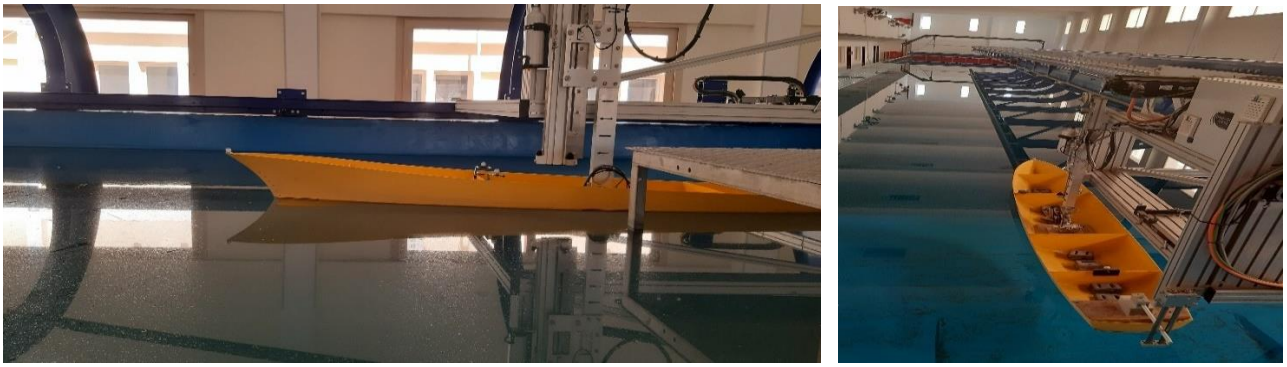

(a) (b)

Fig. 6. (a) DTMB #5415 Model and experimental set up; (b) MTC- Towing Tank

The model was placed in the tank's centre, both longitudinally and transversely. To measure the elevation of the water's surface, a resistance wave gauge controller with eight channels and eight probes was set up. With one resistance probe placed 15 cm from the wave maker and one ultrasonic wave probe close to the model, it was observed and recorded. The mass density and viscosity of water are calculated using the ITTC procedure [20]. Before conducting model testing, the dynamometer was calibrated using masses in accordance with the ITTC Protocol [21].

Systems for signal conditioning and data collection are installed on the driving carriage. To minimize errors in the extension of the ship, the measurement of the model resistance must be exceedingly precise. The most crucial prerequisite for measuring the resistance of a ship model is

consistency of speed for the towing carriage, together with the precision of the resistance dynamometer made by Edinburgh Designs Ltd. in conjunction with a model clamp.

On a Kempf and Remmers accuracy test platform, the load cell, signal conditioner, and carriage PC AD card are statically calibrated to ascertain the voltage-mass relationship. To lessen the sensitivity of the signal to noise, amplified analogue voltages are transformed into frequencies (3000±2500 Hz) for transmission to the AD card [22]. The carriage is driven at the desired constant speed during each test run, and measurements of the speed and model resistance are made to help interpret the data afterwards.

With a 5-camera system properly positioned above the water's surface, the Qualisys video motion capture system was used to measure the model's six degrees of freedom of motion. It is comprised of seven infrared reflectors strategically placed on the vessel (illuminated balls). The coordinates of the balls in 3D space are registered by five cameras suitably positioned near the vessel and the six-degree of freedom motions are calculated and output in real time.

3.2 Construction of the Model

The International Towing Tank (ITTC) has chosen the DTMB 5415 hull shape model as a suggested benchmark naval ship for CFD validation for a resistance study [23]. The model presents a transom stern and a bow bulbous of peculiar shape that allows the sonar lodging. The length between perpendiculars (L_{pp}) of the general tested DTMB model is 5.72 m, which translates to a scale of 24.8. All of the testing was done in bare hull conditions. In our tests, one identically shaped model was tested. It was constructed in the model factory of Edinburgh Designs Ltd. The MTC-TT model is constructed from fiberglass. The main components of the geosim model and the hull lines plan are shown in Table 3 and Figure 7, respectively. The 1:51 model's internal geometry matched that of the ITTC presentation exactly. The four watertight bulkheads have been built on the model, and Figure 8 shows where they are located in relation to ship scale.

Table 3
Main particulars of national US combatant Ship DTMB 5415

Particulars	Ship	Model 24	Model 51
L_{OA} (m)	153.300	6.167	3.0
L_{PP} (m)	142.200	5.72	2.780
B_{OA} (m)	20.540	0.826	0.403
B_{WL} (m)	19.082	0.767	0.375
D (m)	12.470	0.502	0.244
T (m)	6.150	0.248	0.120
V (m^3)	8424.4	0.549	0.0635
Δ (t,kg)	8636	0.549	63.5
KM (m)	9.493	0.382	0.186
KG (m)	7.555	0.304	0.148
GM (m)	1.938	0.078	0.038
LCG (m)	70.137	2.884	1.375
	Hull Coefficient		
C_B	0.505	L_{PP}/B	7.530
C_P	0.616	B/T	3.091
C_M	0.815	C_W	0.778

The model adopted a row of cylindrical studs with a 3 mm height and 3 mm diameter, spaced 30 mm apart, and fitted them 60 mm behind the bow profile in order to promote turbulent flow. The size and spacing of the studs follows [24]. In the following discussion, as well as in the introduction, we refer to the model as DTMB 5415-51.

Tolerances on the model must be kept to a minimum. The waterline at the design draught was free of trim and sinkage, and the surface was correctly completed and ballasted to the required displacement. It was attached to the resistance dynamometer of the towing carriage according to ITTC procedure [25].

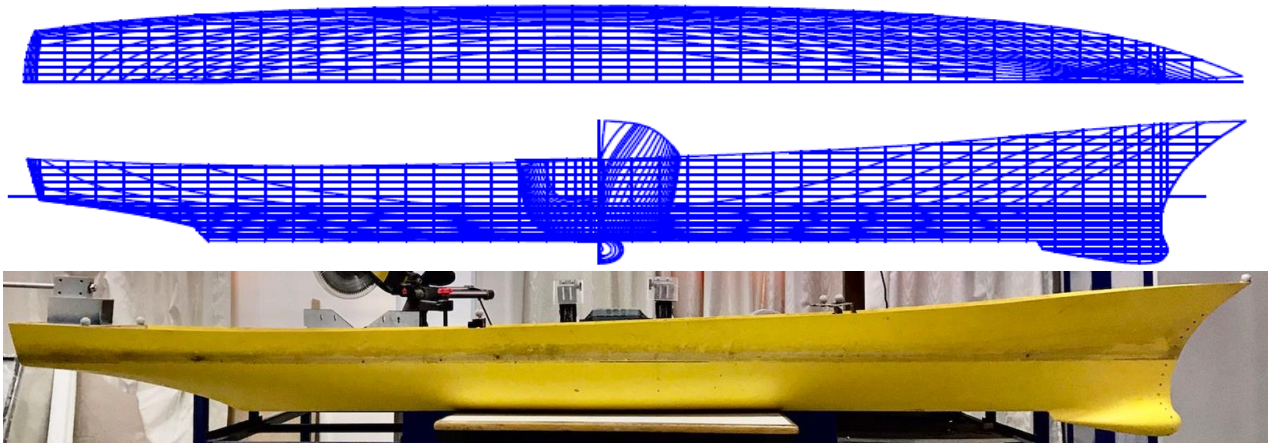

Fig. 7. DTMB #5415 geometry, photo and lines plan

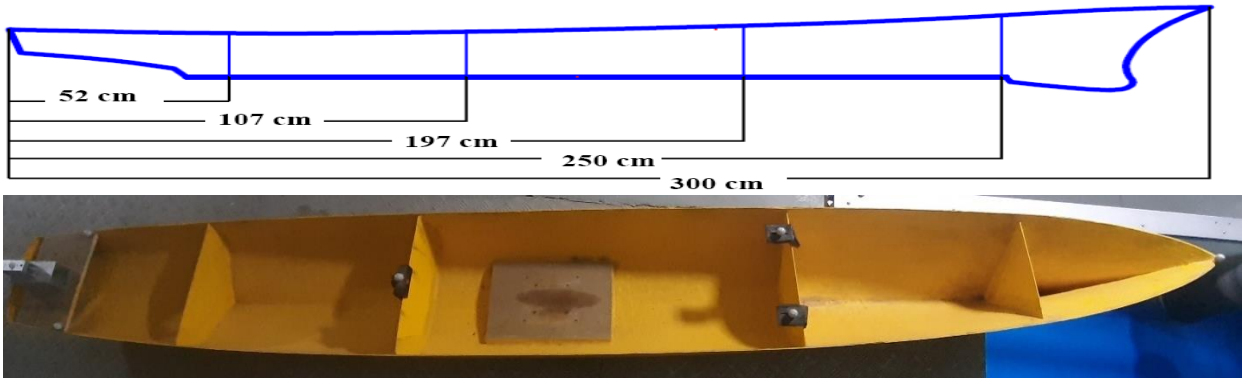

Fig. 8. Model subdivision—dimensions are in ship scale

3.3 Description of Test Conditions and Test Trials - Tests Design

The MTC-TT test used the standard towing tank tests for resistance, sinkage, and trim, and it was conducted as usual [26]. Accuracy assessments are essential for experiments that use processes. An uncertainty analysis was created before to the testing in order to assess the level of accuracy that might be expected from the outcomes. The AIAA rules state that uncertainty analysis is a well-established method for determining if experimental results are accurate and that it should be required at all stages of experimentation [27]. It is helpful for reviewing data obtained for comparing data from many studies throughout the planning and development phases of research. As part of the internal development and application of uncertainty analysis processes and the assessment of scale effects and facility bias, conventional uncertainty assessment procedures are used to determine the data quality [28].

Resistance measurements have been made in free-model settings with Froude numbers ranging from Fr = 0.05 to 0.40, as well as sinkage and trim. The forces have been measured using load cells, while sinkage and trim have been determined using a mechanism that converts encoder-recorded translations into rotations. A forward-perpendicular and design waterplane intersection has been chosen as the origin of a Cartesian coordinate system. The (x, y, and z) axes are oriented in that order (downstream, transverse, and upward) respectively [29].

Towing tank water temperature is measured regularly to allow water viscosity to be estimated for the calculation of Reynolds number and hence friction coefficient at the model mid draft using a digital thermometer as shown in Figure 9. The water data will allow the calculation of viscosity and density, and thus the Reynolds number, for each run. Tests were carried out at water kinematic viscosity v_M = 1.16 x 10^{-6} m^2/s and density 999.2 kg/m^3. The towing force in (kg) is converted to Newtons (N) by multiplication with g=9.81 m/s^2. The resistance values of the ship model are estimated for calm water conditions without the appendages (the rudder and the propeller) [30].

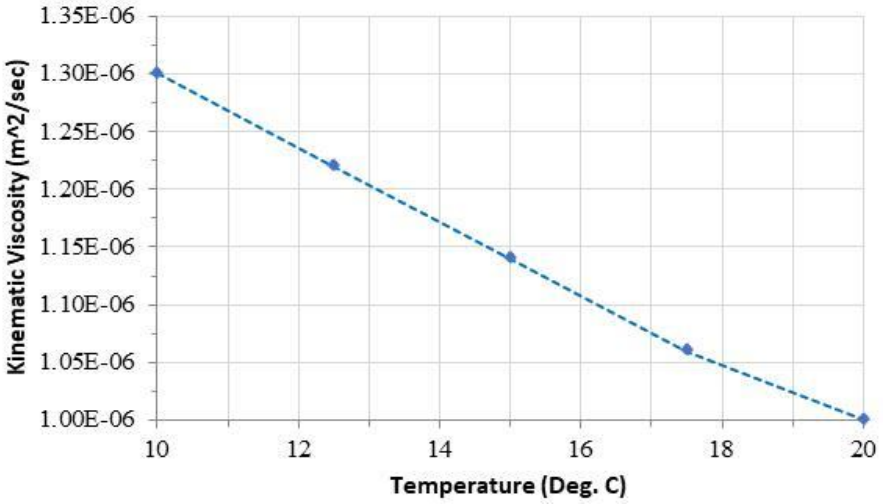

Fig. 9. Viscosity Vs temperature in fresh water

3.4 Setup and Experimental Procedure

The ITTC standards for model speed V_m between 0.1 and 2 m/sec were followed in performing the resistance test. Three experiments were conducted under identical circumstances on different days. To establish the precision limit, ten repeated readings have been taken at V_m = 0.5, 1.0, 1.5, and 2 m/sec. A load cell with a maximum load of 100 N has been used to assess the total model resistance. Before converting from voltage to frequency (V/F), the cell signal was boosted in order to lessen its vulnerability to transmission line noise. As a result, it was sent at a frequency of 3000±2500 Hz, translating to a voltage range of ±5 V, which was then transformed (F/V) into an output voltage for the purpose of acquisition by a 12-bit acquisition board mounted on a computer.

Using the same tools that would eventually be mounted on the carriage for the trials, the load cell calibration was completed [31]. Tachometric equipment has been used to measure the velocity, which the carriage control system has kept at the predetermined value. For every metre of carriage displacement, a tachometric wheel generates 1000 pulses on an optical encoder, yielding a spatial resolution of 0.001 m. The velocity in mm s^{-1} was calculated from the pulses that a 16-bit binary counter counted over a 1 s time. This number is transferred to the acquisition board and shown on the carriage control panel [32].

At the same Froude numbers and resistance, sinkage and trim have been determined by measuring the displacements of two points that are respectively close to the fore and rear perpendiculars [33]. Two angular potentiometers coupled to two pantographs have been used to measure the displacements of the two spots. Due to the very small trim angle, the relationship between fore-and-aft displacements and the trim angle has been linearized [34].

Rotative potentiometers were used to calculate sinkage and trim by measuring fore and aft displacements. Displacement measurements were obtained by converting vertical displacements to angular displacements using weighted, mechanical parallelograms. Potentiometers, signal conditioners, and the carriage PC AD card are statically calibrated to establish the voltage-displacement connection. To obtain the data, 300 discrete samples were collected at a rate of 30 Hz over the course of 10 seconds. A low-pass filter operating at 10 Hz filters the data. The first-order relation has calculated the trim angle by:

$$\theta \cong \frac{\Delta i_{FM} - \Delta i_{AM}}{L_{MM}} \tag{1}$$

where Δi_{FM} and Δi_{AM} are the displacement of the point that are near the fore and aft perpendicular respectively and L_{MM} is the distance between these two points [35]. The displacements of the two points, corresponding to the fore and aft perpendicular, have been obtained knowing their distances from the measurement points by relations:

$$\frac{\Delta i_{FM} - \Delta i_{AM}}{L_{MM}} = \frac{\Delta i_{FP} - \Delta i_{AM}}{L_{MM}+D} \Rightarrow \Delta i_{FP} = \Delta i_{AM} + \frac{L_{MM}+D}{L_{MM}} (\Delta i_{FM} - \Delta i_{AM}) \tag{2}$$

$$\frac{\Delta i_{FM} - \Delta i_{AM}}{L_{MM}} = \frac{\Delta i_{AM} - \Delta i_{AP}}{L_{PP} - L_{MM} - D} \Rightarrow \Delta i_{AP} = \Delta i_{AM} - \frac{L_{PP} - L_{MM} - D}{L_{MM}} (\Delta i_{FM} - \Delta i_{AM}) \tag{3}$$

where D is the separation between the measuring point's front and the front perpendicular. The following relationship has been used to determine sinkage:

$$\Delta i = \frac{1}{2} (\Delta i_{FP} + \Delta i_{AP}) = \left(1 - \frac{L_{PP} - 2D}{2L_{MM}}\right) \Delta i_{FM} + \left(\frac{L_{PP} - 2D}{2L_{MM}}\right) \Delta i_{AM} \tag{4}$$

4. Results and Discussion

4.1 Numerical Calculations

In the first preliminary step, the DTMB 5415-51 model's calm water resistance was tested using CFD against model speeds ranging from 0.25 to 2.3 m/sec, or Fn 0.05 to 0.45. Three different mesh sizes were employed to estimate the hydrodynamic performances for the CFD mesh investigation. To assess the convergence of the solution as depicted in Figure 10, the calculated drag on the hull was measured, plotted, and compared with the Maxsurf results (Holtrop and Mennen method). The findings for the coarse, medium and fine grid results are extremely similar and the difference ε = (medium - coarse) / (fine - medium), where 0< ε <1 is small and acceptable as shown in Table 4 [16] [36].

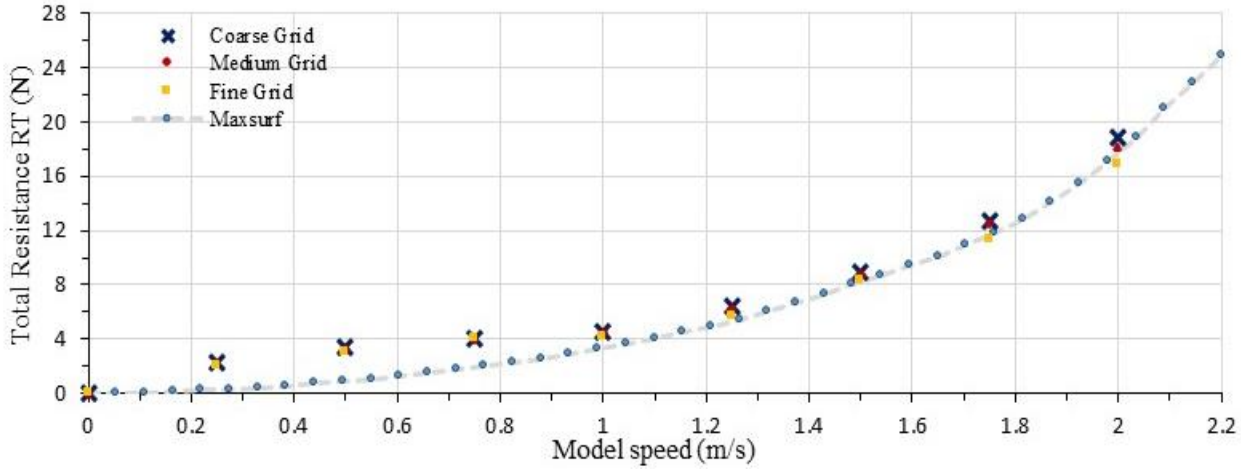

Fig. 10. Resistance curve for DTMB #5415-51 comparing three different sized grids with Maxsurf

Table 4
The CFD results for DTMB 5415-51 model

Vm (m/sec)	0.25	0.5	0.75	1	1.25	1.5	1.75	2
R_T (N) (C)	2.263521	3.391023	4.008125	4.514248	6.392025	8.921542	12.77402	18.84354
R_T (N)(M)	2.152487	3.254165	4.00052	4.45213	6.25418	8.744121	12.54152	18.12484
R_T (N) (F)	1.995422	2.987445	3.985412	4.105481	5.652481	8.312584	11.33254	16.84521
Difference ε	0.706929	0.513115	0.503376	0.179196	0.229093	0.411137	0.192312	0.561648

Figure 11 illustrates the total resistance coefficient for the three grids with speed. According to the bare hull results, the mesh generation approach may be used to estimate hydrodynamic performances using CFD, and convergence of the numerical predictions demonstrates that the overall strategy is appropriate for resistance prediction. The results for the coarse and medium grids are quite similar, and the difference between the medium and fine grids is comparatively bigger but still tolerably tiny. Therefore, the fine grid provides the best match for the calculations and displays the outcomes, which are most appropriate.

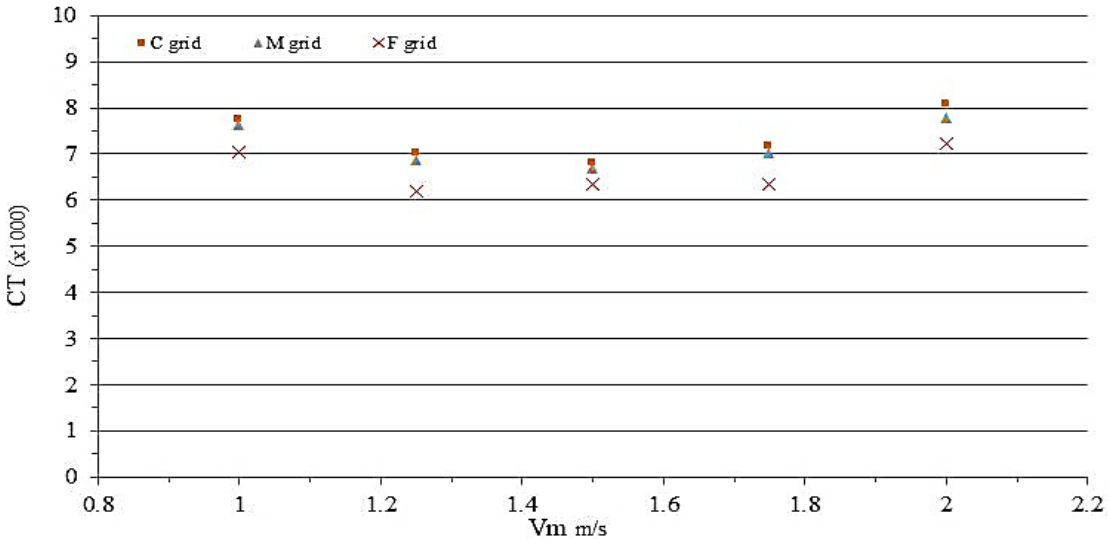

Fig. 11. The curves of total resistance coefficient CT_M for different grids

Figure 12 shows the time histories of the total resistance, at Fr 0.30 for the 125 seconds that the simulation was run. It is possible to see how the graphs behave oscillatorily as a result of the free surface. The resistance values shown in this figure must be multiplied by two since, as previously mentioned, only half of the ship was simulated and the symmetry requirement was applied. The frictional and residuary resistances, into which the total resistance is divided, can also be provided by the CFD code [37]. While the frictional resistance is largely steady, the pressure resistance curve can be seen to oscillate. The oscillations of the pressure resistance values that can be attributed to the effect of the free surface are transmitted to the values of the total resistance[38].

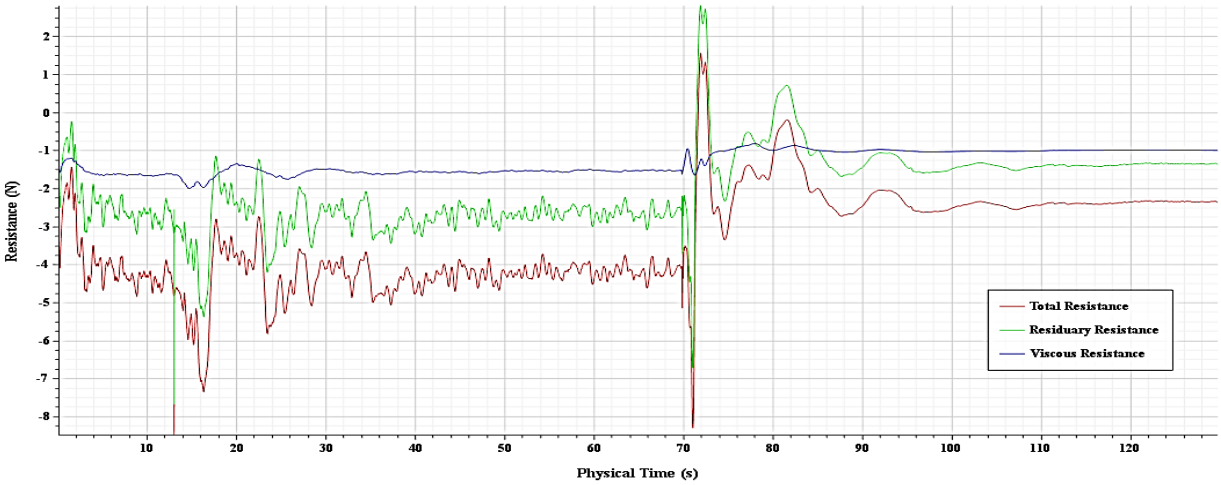

Fig. 12. Time history of resistance as generated in CFD at Fr=0.38

Finally, figures for the hull model's free surface wave and volume fraction (water) contours at various Froude numbers are presented in Figure 13 and 14 respectively.

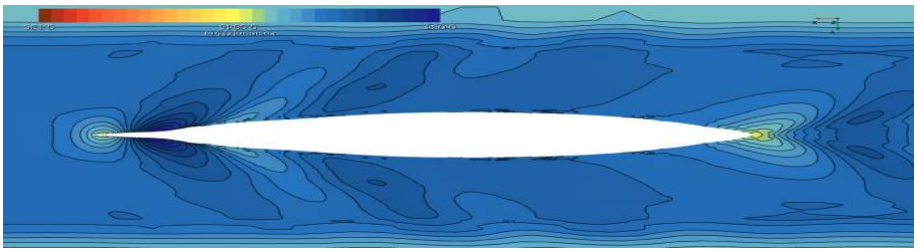

Fig. 13. Wave pattern for bare hull at Fn = 0.40 - coarse grid

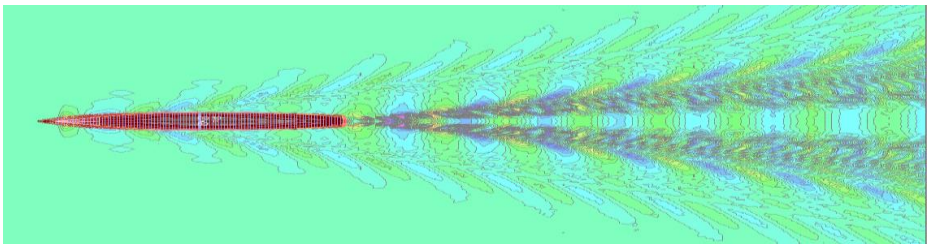

Fig. 14. Free surface wave contours for at Fn=0.40 - medium grid

4.2 Experimental Results; Resistance, Sinkage and Trim

This section analyses and explains the experimental data that was gathered. It is believed that the experimental data comparison is sufficient to provide a thorough understanding of the fundamental traits of the difficult methodologies under investigation. Resistance benchmark experiments were

conducted between July and November 2022 to create reference test settings that would allow for the comparison of experimental results from various tests. The benchmark testing outcomes in calm water were examined and the numerical outcomes were contrasted. Plotting resistance, sinkage, and trim versus speed during the testing is crucial for ensuring that the findings are consistent and repeatable. Target speed, measured speed, resistance, sinkage, trim, and water temperature should all be recorded for each run. Variation of model resistance results (for 10 repeats) should normally lie in a range +/- 0.5 - 2% of the mean.

The total resistance curve as a function of carriage speed is shown in Figure 15. As prescribed by the ITTC comparative tests, there would be used 10 repeat tests on 4 different days at measured speed V_m = 0.5, 1.0, 1.5 and 2.00 m/s, corresponding respectively to Fr = 0.10, 0.24, 0.34 and 0.39, to perform statistical analysis as demonstrated in Figure 16. Before doing any statistical analysis, the total resistance data in the towing tank are adjusted to the nominal speed and converted to the nominal fresh water temperature of 15 degrees Celsius.

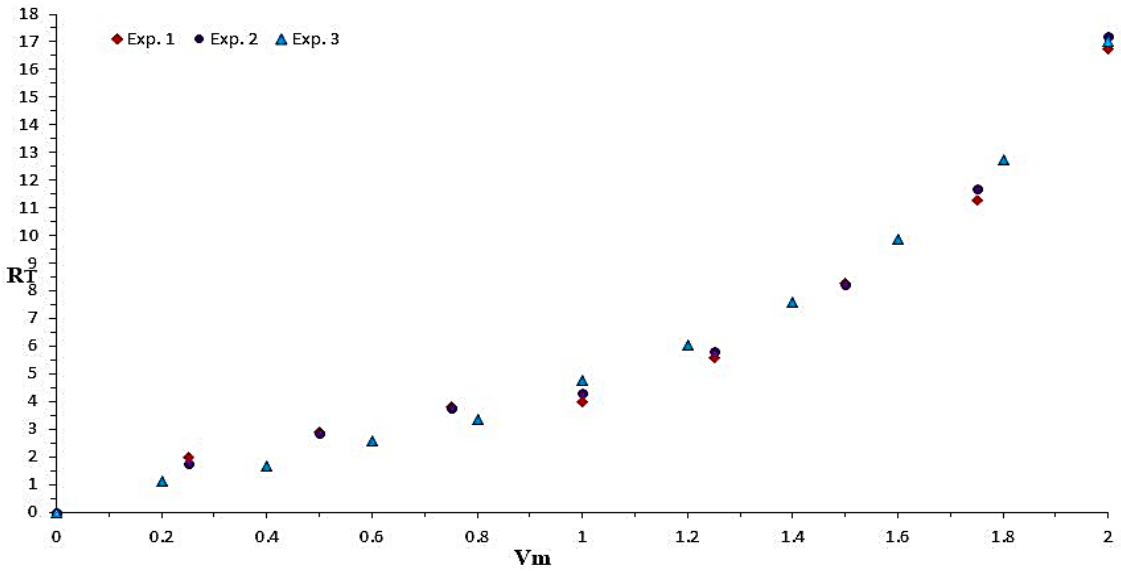

Fig. 15. The total resistance experiment data for DTMB 5415-51

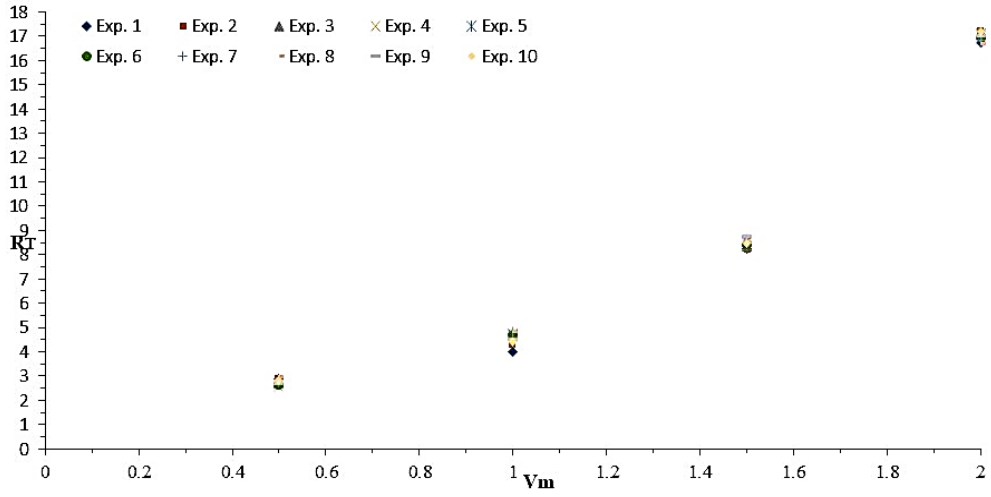

Fig. 16. The total repeat resistance tests for DTMB 5415-51

The means of total resistance from those repeat tests are given in Table 5. Such means can be regarded as the most accurate in each resistance test in the towing tank. The experimental standard deviation (StDev) of tests is also presented. These standard deviations can be used to calculate the measurement's repeatability and uncertainty.

Table 5
Statistical analysis resistance value for hull model

Fr	Mean	StDev	Fr	Mean	StDev	Fr	Mean	StDev
0.15	3.6328	2.16 %	0.24	5.8403	1.07 %	0.34	11.6138	0.98 %
0.19	4.2877	1.33 %	0.29	8.3442	1.92 %	0.39	16.9876	1.21 %

The form factor k is calculated as recommended by the ITTC (1978) using Prohaska's method (ITTC, 1966). The approach assumes that CR can be approximated by the following equation at low speed and without separation:

$$C_W = C_{TM} - C_V = C_{TM} - C_{FM}(1+K) \tag{5}$$

$$\frac{CT}{CF} = (1+K) + \frac{yFr^4}{CF} \tag{6}$$

and values of C_T/C_F form a line with slope y and intercept (1+k). For The hull model, C_T data is used for $0.05 \leq Fr \leq 0.2$, and the results are provided below in Figure 17. The estimated intercept is (1+k)=1.207.

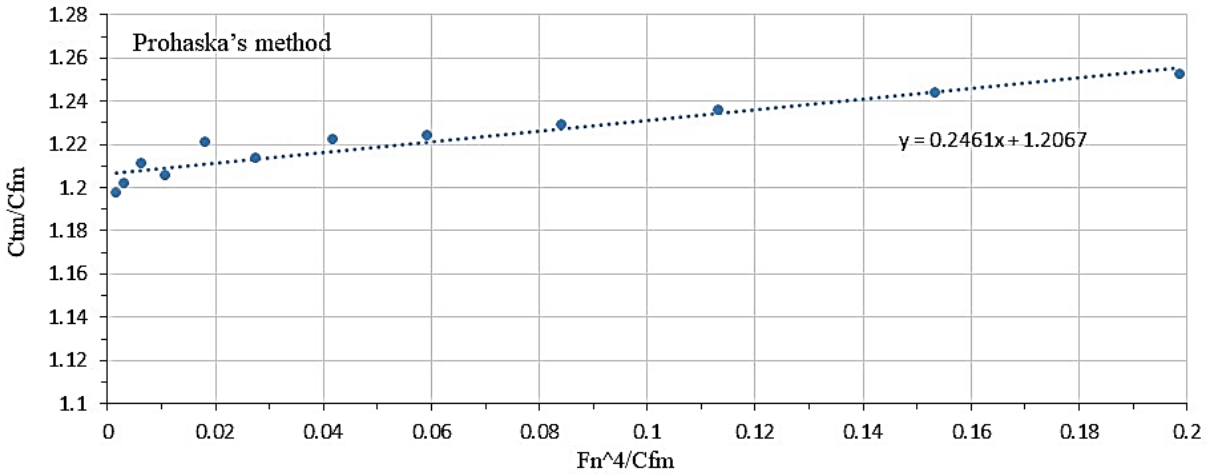

Fig. 17. Evaluation of the form factor for model 5415-51 using Prohaska's method

The graphs of total and residual resistance coefficients (C_{TM} and C_R vs. F_r, respectively, are shown in Figure 18. Also viscous resistance has reported according to the ITTC 57 formula. Even though the model was unloaded and demounted at the end of each day, the data obtained reveal no appreciable dispersion. When Fr is between 0.05 and 0.15, C_{TM} gradually drops, remains constant (C_{TM}=0.005) between 0.15 and 0.225, gradually increases between 0.225 and 0.35, and rapidly increases when Fr is greater than 0.35. For Fr values of 0.1 to 0.225, 0.225 to 0.35, and Fr greater than 0.35, C_R is essentially piecewise linear with a rising slope. The presence of humps and hollows is minimal in both situations.

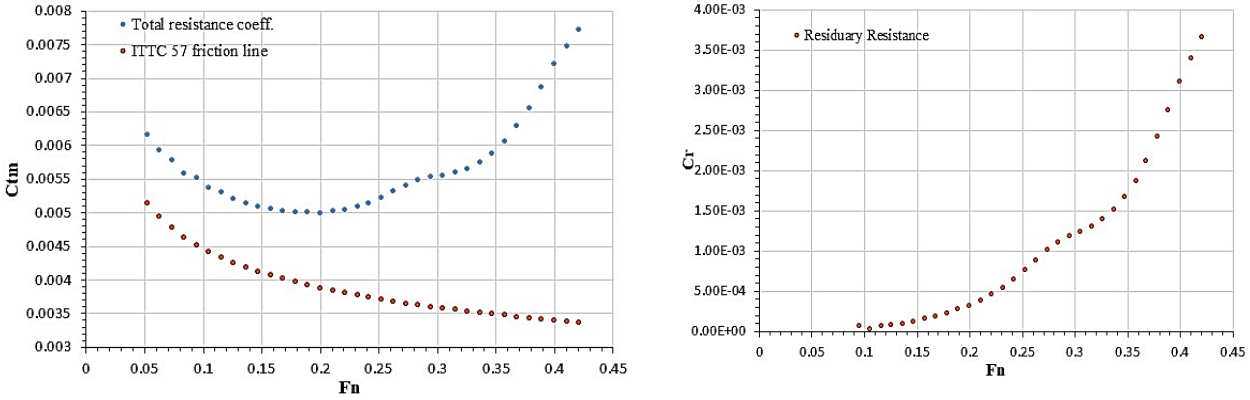

(a) (b)

Fig. 18. (a) The curves of total and (b) residual resistance coefficient C_{TM} and C_R

As a function of carriage speed, a series of towing tests were conducted between Fr = 0.05 and 0.40. The model was allowed to take its natural sinkage and trim angle during the tests. The average of 10 times-repeated experiments yielded the values at Fr = 0.10, 0.20, and 0.30. Sinkage and model resistance have both been measured fore and aft. The sinkage σ and trim τ versus Fr are shown in Figure 19(a) and (b). Model sinkage rises as Fr increases, and she has a weak bow down trim for Fr less than 0.20 and a strong bow up trim for Fr greater than 0.20. σ is roughly linear for 0.1 < Fr < 0.35. For Fr < 0.2, the data is mildly increases, whereas from Fr 0.2 to 0.35, σ rapidly increases. τ is roughly piecewise linear with mild negative slope for 0.1< Fr < 0.26 and increasing positive slope for 0.26 < Fr < 0.4.

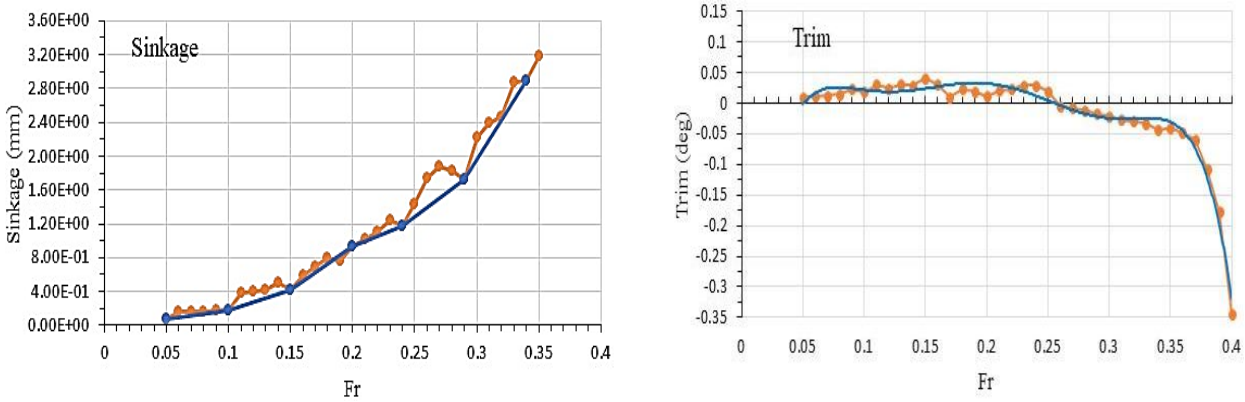

(a) (b)

Fig. 19. Sinkage and trim data for model 5415-51

Figure 20 shows the time resistance chart and the time velocity chart whereas the measured speed and drag vs time at 2 m/sec in MTC-TT are demonstrated in Figure 21.

The wave pattern and the wave outlines along the hull at Fr = 0.30 are shown in Figures 22 and 23 based on data from the towing tank. When it comes to accurately capturing the general shape of the wave pattern, we observe that the towing tank tests are in good agreement with the CFD code.

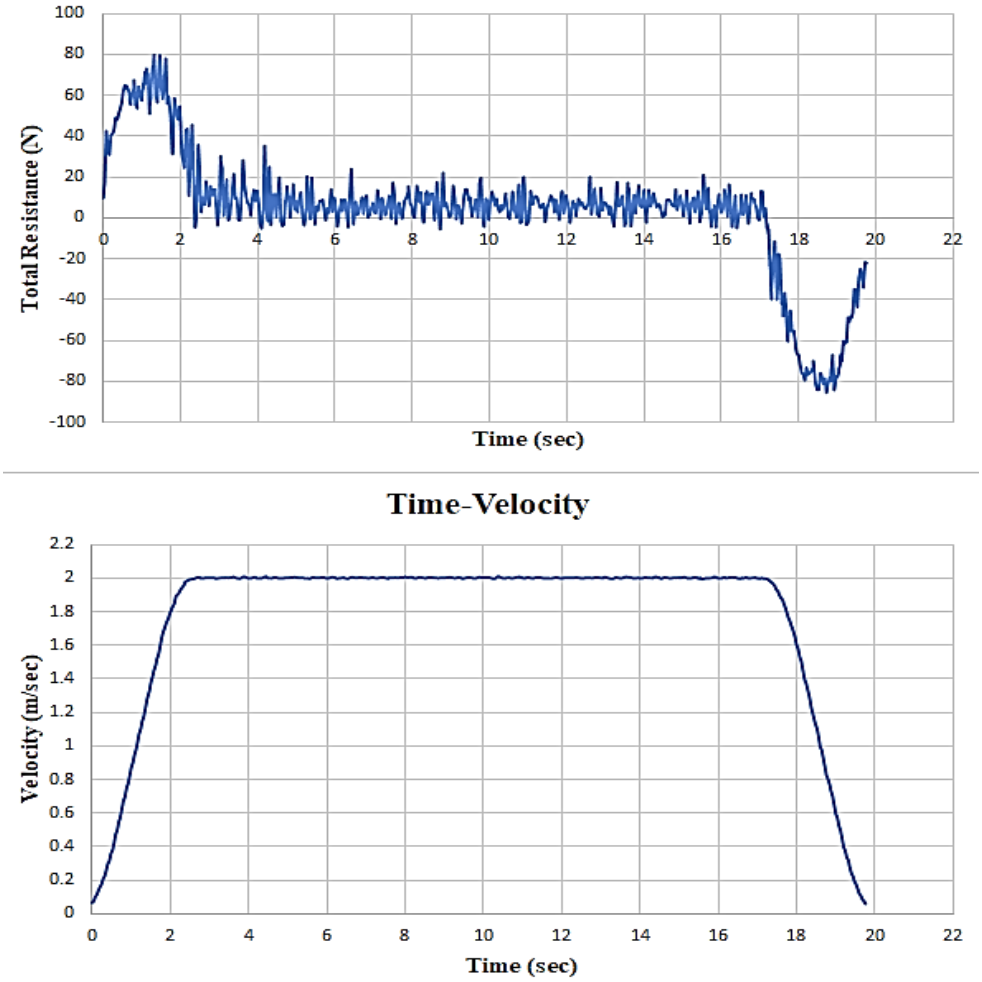

Fig. 20. Time resistance chart – time velocity chart at 2 m/sec

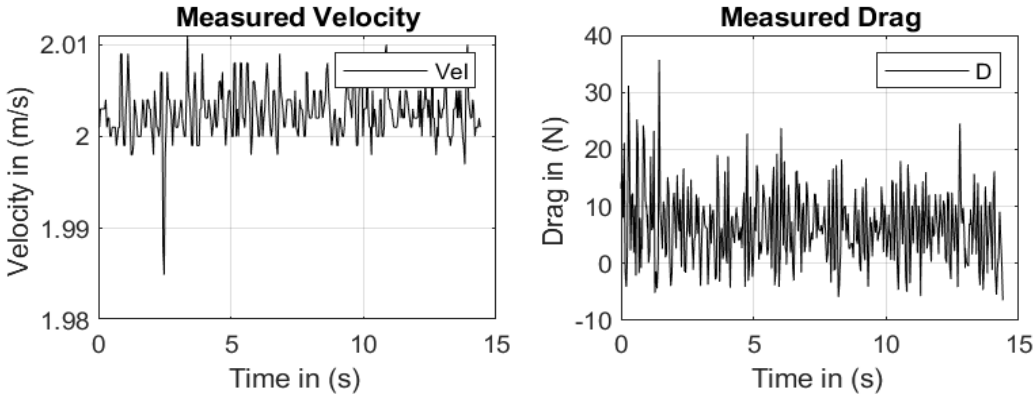

Fig. 21. The measured speed and drag vs time at 2 m/sec in MTC-TT

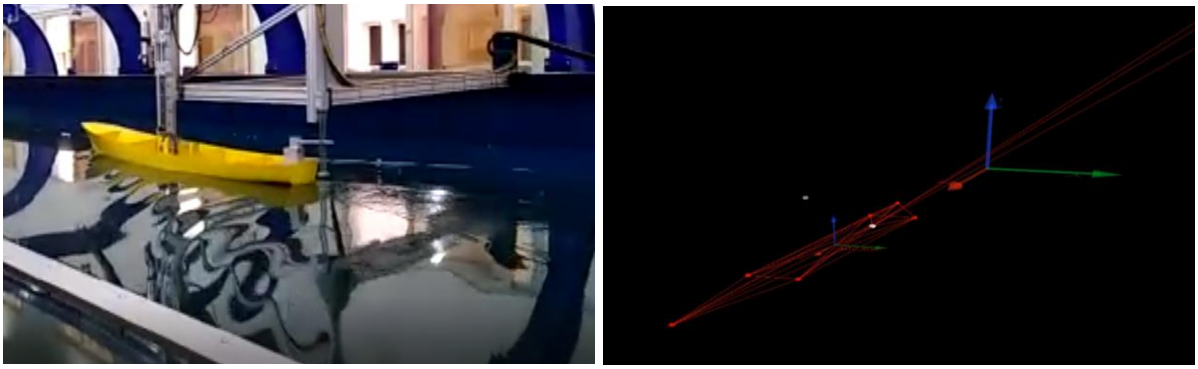

Fig. 22. The wave pattern along the hull at Fr = 0.30

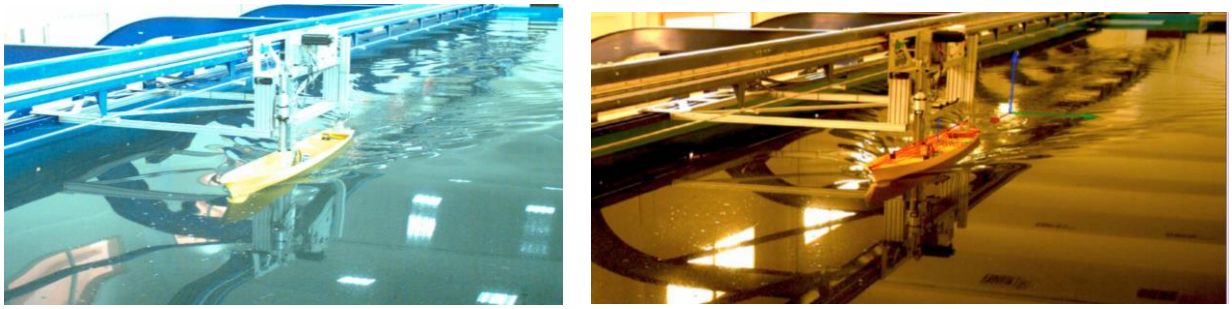

Fig. 23. The wave contours along the hull at Fr = 0.30

Figure 24 shows the CFD results as well as the experimental data from the towing tank for total resistance. As a way of predicting calm water resistance, it offers a graphic representation of the agreement between experimental and CFD values. Table 6 compares the experimental results to the numerical estimates of ship resistance, and the error % is provided by

$$\Delta R_T\% = (R_T^{CFD} - R_T^{exp})/ R_T^{exp}. \quad (7)$$

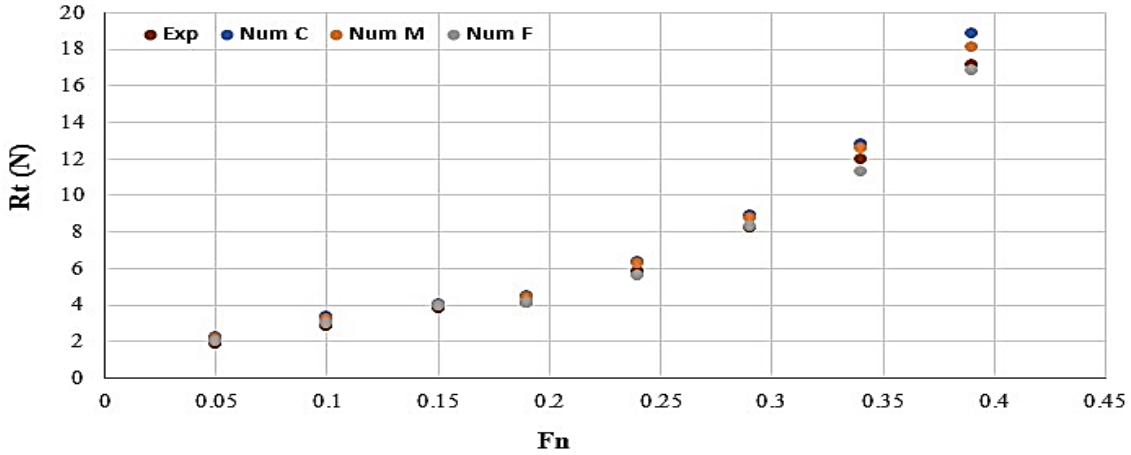

Fig. 24. Total resistance experimental data plotted with CFD results

At lower speeds, the agreement of the calculations from the CFD simulations with the experimental data worsens, and as shown in Table 6, at Fr=0.35, the CFD values deviate significantly from the experimental data. In general, the results show that the resistance values at various speeds for the fine mesh show a very good and improved agreement with the experimental data, with an error of less than 6%. The highest agreement between experimental and computational results is found for total resistance.

Table 6
The comparison of experimental and CFD results for DTMB #5415-51 using different meshes

Fn	V_m (m/s)	R_T (N) (Exp.)	R_T (N) (C) (Simulation)	Δ R_T (%)	R_T (N)(M) (Simulation)	Δ R_T (%)	R_T (N) (F) (Simulation)	Δ R_T (%)
0.05	0.25	1.89269414	2.263521	19.59254	2.152487	13.72609	1.995422	5.4275785
0.1	0.5	2.88282046	3.391023	17.62866	3.254165	12.88129	2.987445	3.6292421
0.15	0.75	3.78658455	4.008125	5.850667	4.00052	5.649826	3.985412	5.2508391
0.19	1	4.153801	4.514248	8.677522	4.45213	7.182073	4.105481	-1.163272
0.24	1.25	5.82283543	6.392025	9.775127	6.25418	7.407809	5.652481	-2.925627
0.29	1.5	8.24017278	8.921542	8.268871	8.744121	6.115748	8.312584	0.8787585
0.34	1.75	11.9915089	12.77402	6.525552	12.54152	4.586672	11.33254	-5.4952956
0.39	2	17.1598606	18.84354	9.811737	18.12484	5.623469	16.84521	-1.8336429

5. Conclusion

The objective of the current study is to contribute to combatant geometry DTMB Model 5415-51's surface-ship resistance, sinkage, and trim. Reliable CFD data is needed for a benchmark test conducted internally. It confirms the significance of such arduous experiments in understanding the behaviour of the flow around the DTMB model. The primary goal of this experiment is to create a useful database for numerical code testing. The model's CFD codes have to undergo a thorough examination in order to verify the experimental results.

A significant portion of the current data set was cross-validated using experimental results obtained at DTMB, yielding a very good result. Extensive comparisons between our CFD calculations and experimental results for DTMB 5415-51 show that the method used is acceptable and that the mesh generation method can be used to estimate the model's hydrodynamic performance. The fine grid will be utilized since it is most appropriate for the calculation and produces the best results because convergent results are achieved as mesh size decreases, according to a comparison of total resistance grid results by CFD. On the other hand the obtained experimental results validated the setup of the towing tank facility and adequacy of procedures.

Acknowledgement
This research was not funded by any grant**.**

References
[1] Zhang, Zhi-rong, Liu Hui, Song-ping Zhu, and Z. H. A. O. Feng. "Application of CFD in ship engineering design practice and ship hydrodynamics." *Journal of Hydrodynamics, Ser. B* 18, no. 3 (2006): 315-322. https://doi.org/10.1016/S1001-6058(06)60072-3
[2] Stern, F., J. Longo, R. Penna, A. Olivieri, T. Ratcliffe, and H. Coleman. "International collaboration on benchmark CFD validation data for surface combatant DTMB model 5415." In *Twenty-Third Symposium on Naval HydrodynamicsOffice of Naval ResearchBassin d'Essais des CarenesNational Research Council*. 2001.
[3] Shia, Aiguo, Ming Wu, Bo Yang, Xiao Wang, and Zuochao Wang. "Resistance calculation and motions simulation for free surface ship based on CFD." *Procedia Engineering* 31 (2012): 68-74. https://doi.org/10.1016/j.proeng.2012.01.992
[4] Żelazny, Katarzyna. "A method of calculation of ship resistance on calm water useful at preliminary stages of ship design." *Zeszyty Naukowe Akademii Morskiej w Szczecinie* 38 (110 (2014): 125-130.
[5] Elhadad, Aladdin, Wen Yang Duan, Rui Deng, and H. Elhanfey. "Numerical Analysis for Resistance Calculations of NPL as a Floating Hull for Wave Glider." *Applied Mechanics and Materials* 619 (2014): 38-43. https://doi.org/10.4028/www.scientific.net/AMM.619.38
[6] Zhao, Feng, Song-Ping Zhu, and Zhi-Rong Zhang. "Numerical experiments of a benchmark hull based on a turbulent free-surface flow model." *Computer Modeling in Engineering and Sciences* 9, no. 3 (2005): 273-285.
[7] ITTC. Resistance Committee 1. Resist Comm 27th ITTC 2014:27–8.
[8] Rosemurgy, William J., Deborah O. Edmund, Kevin J. Maki, and Robert F. Beck. "A Method for resistance prediction

in the design environment." In *11th International Conference on Fast Sea Transportation FAST*. 2011.
[9] Ahmed, Y., and C. Guedes Soares. "Simulation of the flow around the surface combatant DTMB model 5415 at different speeds." In *13th Congress of Intl. Maritime Assoc. of Mediterranean, Istanbul, Turkey*, pp. 307-314. 2009.
[10] Menter, Florian R. "Two-equation eddy-viscosity turbulence models for engineering applications." *AIAA journal* 32, no. 8 (1994): 1598-1605. https://doi.org/10.2514/3.12149
[11] Elhadad, Aladdin, Wen Yang Duan, and Rui Deng. "Comparative investigation of an automated oceanic wave surface glider robot influence on resistance prediction using CFD method." *Applied Mechanics and Materials* 710 (2015): 91-97. https://doi.org/10.4028/www.scientific.net/AMM.710.91
[12] Ahmed, Alaaeldeen Mohamed Elhadad. "Resistance Evaluation for the Submerged Glider System using CFD Modelling." *Journal of Advanced Research in Applied Sciences and Engineering Technology* 29, no. 3 (2023): 147-159. https://doi.org/10.37934/araset.29.3.147159
[13] Rhee Sh. Computational Validation Of Flow Around Surface Ships Using, workshop on CFD ship hydrodynamics, pp. 504-509, March 9-11, Tokyo, Japan, 2005.; 2016.
[14] Diez, Matteo, Andrea Serani, Emilio F. Campana, Omer Goren, Kadir Sarioz, D. Bulent Danisman, Gregory Grigoropoulos et al. "Multi-objective hydrodynamic optimization of the DTMB 5415 for resistance and seakeeping." In *SNAME International Conference on Fast Sea Transportation*, p. D021S005R012. SNAME, 2015. https://doi.org/10.5957/FAST-2015-034
[15] Larsson, Lars, Frederick Stern, and Michel Visonneau. "CFD in ship hydrodynamics—results of the Gothenburg 2010 workshop." In *MARINE 2011, IV International Conference on Computational Methods in Marine Engineering: Selected Papers*, pp. 237-259. Springer Netherlands, 2013. https://doi.org/10.1007/978-94-007-6143-8_14
[16] Jones, D. A., and D. B. Clarke. *FLUENT Code simulation of flow around a naval hull: the DTMB 5415*. 2010.
[17] Nasirudin, Ahmad, I. Ketut Aria Pria Utama, and Andreas Kukuh Priyasambada. "CFD Analysis into the Resistance Estimation of Hard-Chine Monohull using Conventional against Inverted Bows." *CFD Letters* 15, no. 6 (2023): 54-64. https://doi.org/10.37934/cfdl.15.6.5464
[18] Pacuraru, F. "Validation of potential flow method for ship resistance prediction." In *IOP Conference Series: Materials Science and Engineering*, vol. 591, no. 1, p. 012113. IOP Publishing, 2019. https://doi.org/10.1088/1757-899X/591/1/012113
[19] ITTC, ITTC. "Recommended procedures and guidelines." *Resistance Test* (2011).
[20] Olivieri, A., F. Pistani, A. Avanzini, F. Stern, and R. Penna. "Towing tank experiments of resistance, sinkage and trim, boundary layer, wake, and free surface flow around a naval combatant INSEAN 2340 model." *Security* 421 (2001): 1-42. https://doi.org/10.5957/ATTC-2001-019
[21] Begovic, Ermina, A. H. Day, and Atilla Incecik. "Experimental ship motion and load measurements in head and beam seas." In *9th Symposium in High SPeed Marine Vehicles*. 2011.
[22] Pedersen, Torstein, Sven Nylund, and A. Dolle. "Wave height measurements using acoustic surface tracking." In *OCEANS'02 MTS/IEEE*, vol. 3, pp. 1747-1754. IEEE, 2002.
[23] ITTC. Ship Models – 7.5-01-01-01. 23th Int Towing Tank Conf 2002:266–73.
[24] Toda, Y., F. Stern, I. Tanaka, and V. C. Patel. "Mean-flow measurements in the boundary layer and wake of a series 60 CB= 0.6 model ship with and without propeller." *Journal of Ship Research* 34, no. 04 (1990): 225-252. https://doi.org/10.5957/jsr.1990.34.4.225
[25] Andersson, Jennie, Marko Hyensjö, Arash Eslamdoost, and Rickard Bensow. "CFD simulations of the Japan bulk Carrier test case." In *Proceedings of the 18th Numerical Towing Tank Symposium. Cortona, Italy*. 2015.
[26] Purnamasari, D., I. K. A. P. Utama, and I. K. Suastika. "Comparative Resistance Test Between Two Towing Tanks (A Case Study at ITS and IHL)." In *Proceeding of the 14th International Conference on QIR (Quality in Research) ISSN*, vol. 1411, p. 1284. 2017.
[27] Purnamasari, Dian, I. Ketut Aria Pria Utama, and Ketut Suastika. "Benchmark study of ship model resistance test." *Applied Mechanics and Materials* 874 (2018): 114-120. https://doi.org/10.4028/www.scientific.net/AMM.874.114
[28] Hakan Ozdemir, Yavuz, Baris Barlas, Tamer Yilmaz, and Seyfettin Bayraktar. "Numerical and experimental study of turbulent free surface flow for a fast ship model." *Brodogradnja: Teorija i praksa brodogradnje i pomorske tehnike* 65, no. 1 (2014): 39-54. ITTC.
[29] ITC The Resistance Committee. Proc 28th ITTC 2017.
[30] ITTC. Fresh Water and Seawater Properties - 7.5-02-02-01.02. 26th Int Towing Tank Conf Rio Jenerio, Brazil, 28 August - 3 Sept 2011:1–45.
[31] Date E. ITTC – Recommended Procedures and Guidelines ITTC Quality System Manual Recommended Procedures and Guidelines Example for Uncertainty Analysis of Resistance Tests in Tow- ing Tanks ITTC – Recommended Procedures and Guidelines 2014.
[32] Mohamad, Salaheldin Ahmed, Alaaeldeen Mohamed Elhadad Ahmed, and Xiqun Lu. "Influence of Macro-Scale

Cylinder Liner Partial Surface Texturing on the Tribological Behavior of Two-Stroke Marine Diesel Engine Piston Ring." *Journal of Advanced Research in Fluid Mechanics and Thermal Sciences* 101, no. 2 (2023): 111-120. https://doi.org/10.37934/arfmts.101.2.111120

[33] Gourlay, Tim P., Jeong Hun Ha, Philipp Mucha, and Klemens Uliczka. "Sinkage and trim of modern container ships in shallow water." In *Australasian Coasts & Ports Conference*, vol. 2015, p. 22nd. 2015.

[34] Sun, Jianglong, Haiwen Tu, Yongnian Chen, De Xie, and Jiajian Zhou. "A study on trim optimization for a container ship based on effects due to resistance." *Journal of Ship Research* 60, no. 01 (2016): 30-47. https://doi.org/10.5957/jsr.2016.60.1.30

[35] Sherbaz, Salma, and Wenyang Duan. "Ship trim optimization: assessment of influence of trim on resistance of MOERI container ship." *The Scientific World Journal* 2014 (2014). https://doi.org/10.1155/2014/603695

[36] Akbarzadeh, Pooria, Pouya Molana, and Mohammad Ali Badri. "Determining resistance coefficient for series 60 vessels using numerical and experimental modelling." *Ships and Offshore Structures* 11, no. 8 (2016): 874-879. https://doi.org/10.1080/17445302.2015.1081779

[37] De Luca, Fabio, Simone Mancini, Salvatore Miranda, and Claudio Pensa. "An extended verification and validation study of CFD simulations for planing hulls." *Journal of Ship Research* 60, no. 02 (2016): 101-118. https://doi.org/10.5957/jsr.2016.60.2.101

[38] Bryant, Daniel John Ebrahim, and K. C. Ng. "Numerical Modelling of Hydraulic Jump Using Mesh-based CFD method and Its Comparison with Lagrangian Moving-Grid Approach." *Journal of Advanced Research in Micro and Nano Engineering* 10, no. 1 (2022): 1-6.